ApJ Letters, in press (June 2001)
Preprint typeset using LaTeX style emulateapj v. 14/09/00

INFRARED SURFACE BRIGHTNESS FLUCTUATIONS OF THE COMA ELLIPTICAL NGC 4874 AND THE VALUE OF THE HUBBLE CONSTANT[1]

Michael C. Liu[2] and James R. Graham
Astronomy Department, University of California, Berkeley, CA 94720
mliu@ifa.hawaii.edu
ApJ Letters, in press (June 2001)

ABSTRACT

We have used the Keck I Telescope to measure K-band surface brightness fluctuations (SBFs) of NGC 4874, the dominant elliptical galaxy in the Coma cluster. We use deep *HST* WFPC2 optical imaging to account for the contamination due to faint globular clusters and improved analysis techniques to derive measurements of the SBF apparent magnitude. Using a new SBF calibration which accounts for the dependence of K-band SBFs on the integrated color of the stellar population, we measure a distance modulus of 34.99 ± 0.21 mag (100 ± 10 Mpc) for the Coma cluster. The resulting value of the Hubble constant is 71 ± 8 km s^{-1} Mpc^{-1}, not including any systematic error in the *HST* Cepheid distance scale.

Subject headings: distance scale — galaxies: distances and redshifts — galaxies: elliptical and lenticular, cD — galaxies: individual (NGC 4874) — infrared: galaxies

1. INTRODUCTION

The Coma cluster (Abell 1656) is an important rung in the cosmic distance ladder. It is the nearest of the very rich Abell clusters (richness class of 2 [Abell 1958]) and thus contains many luminous galaxies which can be targeted for distance measurements. Also, the cluster redshift ($\approx$7000 km s^{-1}) is large enough that its cosmological recession is not significantly perturbed by smaller-scale peculiar velocities (e.g. Strauss & Willick 1995). For both these reasons, several methods have been used to measure the distance to Coma and thereby determine the Hubble constant (H_0). These include Type Ia supernovae (Capaccioli et al. 1990), the Tully-Fisher relation (Giovanelli et al. 1998), the Fundamental Plane (Jorgensen et al. 1995; D'Onofrio et al. 1997), the globular cluster luminosity function (e.g., Kavelaars et al. 2000), and surface brightness fluctuations (Thomsen et al. 1997; Jensen et al. 2001).

Surface brightness fluctuations (SBFs) are an appealing distance indicator because they have a well-understood physical basis — they arise from Poisson statistical fluctuations in the number of stars in a resolution element (i.e., the seeing disk). Over the past decade, optical SBFs have been used to measure distances to elliptical galaxies and the bulges of spiral galaxies (Jacoby et al. 1992; Blakeslee et al. 1999). I-band (0.8 μm) SBFs vary between galaxies by up to one magnitude, but the variations are well-correlated with $V-I_c$ color so they can be compensated. More recently, near-infrared (IR) SBFs have been shown to be useful distance indicators. Because cool giant stars dominate the spectral energy distributions of ellipticals, SBFs are brighter in the near-IR and hence can be detected at greater distances. Unresolved globular clusters are the dominant contaminant for SBF measurements at large distances, but since the clusters are bluer than the old stars in ellipticals, the contamination is much smaller at IR wavelengths. K-band (2.2 μm) SBFs have been measured for galaxies in several clusters (Luppino & Tonry 1993; Pahre & Mould 1994; Jensen et al. 1998, 1999; Mei et al. 2001; Liu et al. 2001).

The core of the Coma cluster is dominated in luminosity by two supergiants, the elliptical NGC 4889 (B_T = 12.53 mag) and the cD NGC 4874 (B_T = 12.63 mag; de Vaucouleurs et al. 1991). Like many Abell clusters, Coma possesses significant substructure (e.g., Davis & Mushotzky 1993; Mohr et al. 1993). However, NGC 4874 appears to be special for two reasons: it is located at peak of the diffuse X-ray emission (White et al. 1993), and it has a strong nuclear radio source characteristic of many central giant ellipticals (Harris 1987). Therefore, it is considered to reside at the heart of the gravitational potential of the cluster (Baier et al. 1990; Colless & Dunn 1996).

In this paper, we measure the distance to NGC 4874 using K-band SBFs. We have recently developed new theoretical models for SBF studies (Liu et al. 2000, hereinafter Paper I). Also, we have completed a new calibration of K-band SBFs using a large sample of early-type galaxies in nearby clusters (Liu et al. 2001, hereinafter Paper II). We have found that K-band SBFs vary considerably between galaxies but, like I-band SBFs, do so in a predictable fashion as they are correlated with $V-I_c$ galaxy color. In this paper, we use these results with new SBF data from the Keck I Telescope to derive an accurate distance to NGC 4874 and consequently a measurement of H_0.

2. OBSERVATIONS

We observed NGC 4874 at the 10-meter Keck I telescope using the facility instrument NIRC (Matthews & Soifer 1994) with the standard K-band filter (2.0–2.4 μm). The camera uses a Santa Barbara Research Corporation 256 $\times$ 256 InSb array and has a $38'' \times 38''$ field. Table 1 summarizes the observations. Both runs were photometric, with

[1] Based in part on observations obtained at the W.M. Keck Observatory, which is operated as a scientific partnership among the California Institute of Technology, the University of California, and the National Aeronautics and Space Administration.

[2] Currently Beatrice Watson Parrent Fellow, Institute for Astronomy, University of Hawai'i, 2680 Woodlawn Drive, Honolulu, HI 96822.

0.″5 FWHM seeing. Images on the galaxy were interlaced with blank sky fields and taken in an ABBA pattern.

We obtained wider-field K'-band (1.9–2.3 μm) images on 28 June 1995 UT using the facility near-IR camera LIRC2 (Gilmore et al. 1995) on the Shane 3-m telescope at Lick Observatory. LIRC2 employs a Rockwell International 256×256 HgCdTe NICMOS-3 array and has a plate scale of 0.″38 pixel^{-1}. Data were obtained in a similar fashion as the Keck data, taking interlaced pairs of sky and galaxy images. Conditions were photometric with a typical seeing FWHM of 1.″1. For all the runs we observed the faint IR standards of Casali & Hawarden (1992) as flux calibrators. Hence, our resulting magnitudes are Vega-based.

Details of the data reduction appear in Paper II. We subtracted an average bias from the images. Using twilight sky images, we constructed flat fields with an iterative-fitting algorithm which separated the flat field from the non-uniform thermal emission on the array. A preliminary sky subtraction was performed to identify astronomical objects. Then for each image, we made a running sky frame from the prior and subsequent images of blank sky, excluding any astronomical objects. The sky brightness changes temporally so we scaled the running sky frames to the median counts in unsubtracted galaxy images, excluding a circular region centered on the galaxy. We used the same masks for scaling the subtraction of the blank sky images. This ensured the blank sky images and galaxy images were reduced identically. NIRC images of bright sources suffer from "bleeding": they have a positive horizontal trail which exponentially weakens along the readout sequence. We used images of bright stars to model the bleeding and remove it. We also used a software mask to exclude a faint in-focus ghost of the exit pupil (the secondary mirror) present in all the images. We used the galaxy to register the individual frames and averaged to assemble a final mosaic.

Finally, we used the Lick images to determine the remaining DC sky background in the Keck images. Being a cD-type galaxy, NGC 4874 has a rather shallow light profile; hence the common technique of assuming the galaxy follows a de Vaucouleurs $r^{1/4}$ profile is ill-suited. We extracted azimuthally averaged profiles from the Lick and Keck images, and fitted for the DC level in the Keck images. To estimate the offset between the slightly different Lick and Keck filters, we used spectra of solar-metallicity M0–M5 giants from Pickles (1998), which should be well-suited for this purpose (Frogel et al. 1978). Our synthesized $(K' - K)$ color was -0.015 ± 0.003 mag, including accounting for the filters' k-corrections at the redshift of Coma.[3] We checked our final calibrated images against the photometry of Persson et al. (1979) taken in a 14.″9 diameter aperture. The agreement was excellent, with our photometry being on average 0.014 ± 0.008 mag brighter.

3. SBF MEASUREMENTS

Our SBF measurement methods are similar to Tonry et al. (1990). A complete discussion appears in Paper II.

The mean surface brightness of NGC 4874 was modeled by fitting for the harmonic content of isophotes. Globular clusters and background galaxies fainter than the detection limit are unresolved point sources in our images. Therefore, they contribute to the fluctuations of the galaxy surface brightness. The effect is substantial, because nearly the entire globular cluster population of the galaxy is unresolved in the K-band images (see below). In order to avoid this contamination, we identified the positions of the globular clusters in our K-band data using archival deep *HST* V-band imaging of NGC 4874 (Kavelaars et al. 2000), which reach down to the peak ($V \approx 27.9$ mag) of the globular cluster luminosity function (GCLF).

We then constructed a software mask defining an annular region and excluding the globular clusters. For the 1998 Keck data, we used two annuli, 3–9″ and 9–12″, chosen to have comparable area. The 1995 Keck data are of lower quality: the total integration was shorter, and at the time the instrument had much higher noise. Therefore, we used only the 3–9″ annulus for this data. The model-subtracted galaxy image was multiplied by this mask, and the Fourier power spectrum of the central 256×256 pixel region determined.

The power spectrum of the model-subtracted galaxy image has two components: (1) rising power at low wavenumbers due to the fluctuations convolved by the point spread function (PSF), and (2) white noise due to the Poisson shot noise. The power spectrum $P(\mathbf{k})$ can be represented as

$$P(\mathbf{k}) = P_0 \times E(\mathbf{k}) + P_1, \qquad (1)$$

where P_0 is the total variance per pixel, P_1 is white noise, and $E(\mathbf{k})$ is the expectation power spectrum. $E(\mathbf{k})$ is the convolution of the PSF power spectrum with the power spectrum of the software mask times the square-root of the galaxy model. It accounts for the PSF, the radial variation in the SBFs, and the effect of the software mask on $P(\mathbf{k})$ (see Liu 2000). Using $E(\mathbf{k})$, we fitted the two-dimensional power spectra to solve for P_0 and P_1 (Fig. 1).

For the very lowest wavenumbers, flat-fielding and sky-subtraction errors produce extra power which contaminates the SBF signal. We examined the power spectra of the blank sky fields, which were observed and reduced in an identical fashion to the galaxy images. We found that wavenumbers of $k \lesssim 20$ (0.08 pixel^{-1}), corresponding to spatial scales of $\gtrsim 4\times$ FWHM, had significant rising power. Therefore, we used only $k = 20$ to $k = 128$, the Nyquist frequency, when fitting the galaxy power spectra.

We analyzed the power spectrum of each quadrant of the galaxy image independently. We used the average of these four fits to obtain P_0 and computed the standard error as the uncertainty in P_0. In Paper II, we ran Monte Carlo tests to verify that these quadrant-derived errors are accurate. Each Keck data set had only one suitable PSF star. Thus we adopted a PSF mismatch error of 0.08 mag, which we determined in Paper II from our Fornax cluster sample.

P_0 is the sum of the variance from the galaxy's stars, which is the desired signal, along with the variance from unresolved astronomical sources and instrumental effects. We quantified the effect of unresolved globular clusters

[3] Our synthesized color is notably different than what would result from the transformation given in Wainscoat & Cowie (1992), which is $K' - K = (0.18 \pm 0.04)(H - K)$. However, as they point out, their transformation was derived from a sample of A stars and M dwarfs. Neither of these have the strong 2.3 μm CO absorption band seen in giant stars, which dominate the near-IR light of elliptical galaxies. The CO feature is within the standard K-band filter, but not in the K'-band filter; hence, the sign of our synthesized correction is as expected.

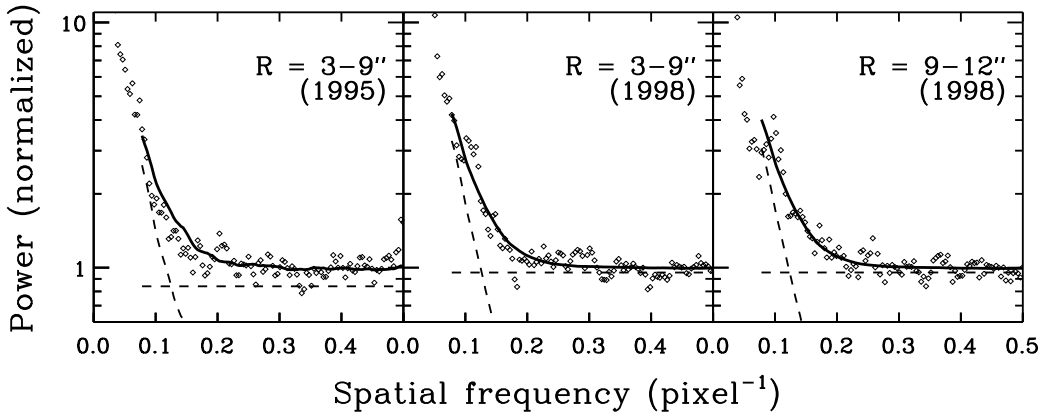

FIG. 1.— K-band fluctuation power spectra for NGC 4874. The galaxy power spectra were fitted by the sum (solid line) of a scaled version of the PSF ($P_0 \times E(k)$) and a constant (P_1); the dashed lines show the contributions from these two components. We did the fit with the two-dimensional power spectra, using spatial frequencies of 0.08 pixel^{-1} to the Nyquist frequency. One-dimensional azimuthal averages are plotted to represent the results, with the measurement annuli and year of observation labeled.

using an analytic representation for the GCLF, namely a Gaussian with three parameters (width, peak magnitude, and normalization) as measured by Kavelaars et al. (2000) using the *HST* V-band data. To convert to K-band, we adopted a color of V–$K = 2.28$, the average of the M31 and Milky Way globular clusters (Barmby et al. 2000). (The optical colors of the NGC 4874 clusters are similar to the Milky Way population, being relatively blue and having a moderately narrow dispersion [Harris et al. 2000].) We then computed the variance per pixel due to the globular clusters below the detection limit of the *HST* optical images, σ^2_{GC}, using eqn. 5 of Blakeslee & Tonry (1995). Note that without the *HST* data, the variance from the undetected globular clusters would be comparable to that from the stellar SBFs, the signal we seek.

Instrumental signatures from flat-fielding and sky subtraction errors add variance to the lowest wavenumbers. By restricting our fits to $k \geq 20$, we reduced the systematic errors. However, these effects might still contaminate the fitting, since they are not step functions in the power spectrum. This is particularly true for NIRC, which has spatially complex flat fields and bias frames. To quantify the amount of leakage into the wavenumbers used for fitting, we used the same techniques on the blank sky fields and measured the blank sky variance per pixel σ^2_{sky} at numerous locations on the images. We used the scatter in the results to find the error in σ^2_{sky}, around 10–15%. While most of σ^2_{sky} arises from instrumental signatures, some comes from real astronomical sources, namely background galaxies fainter than the detection limit. Therefore, unlike the usual SBF analysis, there was no need to compute the residual variance due to unresolved galaxies as this was included in σ^2_{sky}. (Using the counts of Bershady et al. 1998, the variance from the galaxies is predicted to amount to ≈10% of the total variance.)

Finally, the total amplitude of the power spectrum P_0 was corrected by subtracting the contaminating variance P_r. The quantity P_r is the sum of P_{GC} and P_{sky}, which are σ^2_{GC} and σ^2_{sky} divided by the mean galaxy surface brightness per pixel in the measurement region, respectively. The exceptional depth of the *HST* optical data meant that residual variance from the unmasked globular clusters was negligible (≈0.002 mag). The blank sky variance was substantial, about half of the total variance measured in the galaxy images. However, the measurements appear to be robust. For the 1998 Keck data, σ^2_{sky} measured in the two different annuli showed excellent agreement. In the 1995 Keck data, σ^2_{sky} was substantially larger as expected by the higher noise levels then. After subtracting this variance, the resulting K-band SBF apparent magnitude ($\overline{m}_K$) agrees well with those from the 1998 data.

The remaining quantity ($P_0 - P_r$) is the variance due solely to the stellar SBFs. To convert to $\overline{m}_K$, we used the measured photometric zero point and applied two corrections. We corrected for 0.003 mag of extinction (Schlegel et al. 1998). Using the solar-metallicity models of Paper I, we also applied very small k-corrections to $\overline{m}_K$ and $V - I_c$ to account for the redshifting of the galaxy light. The final errors on $\overline{m}_K$ comprise the quadrature sum of the errors in the photometric calibration (0.02 mag), PSF uncertainty (0.08 mag), and measurement errors in the variances (σ^2_{GC}, σ^2_{sky}, and P_0). Table 1 presents our results.

4. RESULTS

In order to compute the distance modulus, we use our K-band SBF calibration from Paper II. This calibration uses 24 early-type galaxies in nearby clusters with high-quality SBF data; the zero point is based on I-band SBF distances to the bulges of six nearby luminous spiral galaxies (Tonry et al. 2000) which have *HST*-derived Cepheid distances from Ferrarese et al. (2000). (The effect of using the new Cepheid distances by Freedman et al. 2001 is ∼0.05 mag — see Paper II.) The calibration is for the K_S-band (2.0–2.3 μm; McLeod et al. 1995) filter, which has a slightly bluer bandpass than the K-band filter used here. To estimate the effect of this difference, we use the theoretical models of Paper I with ages of 3–12 Gyr and metallicities of solar and slightly sub-solar ($Z = 0.02$ and 0.008); these span the SBF observations to date (Papers I and II). The mean ($K_S - K$) offset is effectively zero (0.004 mag) with an rms of 0.02 mag. Thus, we assume no difference but include the rms as an additional source of error. The resulting calibration of the K-band SBF absolute magni-

tude is:

$$\overline{M}_K = (-5.84 \pm 0.04) + (3.6 \pm 0.8)[(V-I_c)_0 - 1.15] \ . \quad (2)$$

This gives us the expected $\overline{M}_K$ for NGC 4874 given its (k-corrected) $V-I_c$ color. A weighted average of the distance moduli from the three data sets is 34.99 ± 0.15 mag. However, the intrinsic (cosmic) scatter about the mean relation is non-zero; in Paper II, we conservatively estimated it to be 0.15 mag. We add this in quadrature to determine a final distance modulus of 34.99 ± 0.21 mag (100 ± 10 Mpc).

Our errors do not include any systematic errors in the *HST* Cepheid distance scale. There are several potential sources of error including the assumed distance to the Large Magellanic Cloud, the metallicity dependence of the Cepheid period-luminosity relation, and the photometric calibration of the *HST* WFPC2 instrument. Any changes in the *HST* Cepheid scale will affect our results by changing the K-band SBF calibration.

Our result is comparable to previous K-band SBF determinations of the distance to Coma. Thomsen et al. (1997) used I-band observations from *HST* to derive a distance of 102 ± 14 Mpc to the Coma elliptical NGC 4881. Jensen et al. (1999) measured a K-band SBF distance of 85 ± 10 Mpc to the other Coma supergiant galaxy NGC 4889. Both of these previous results were based on observations with much lower S/N, $(P_0 - P_r) < 0.7P_1$, at least a factor of 10 worse than our measurements here.

To determine H_0, we adopt a mean velocity for the Coma cluster in the reference frame of the cosmic microwave background of 7186 ± 428 km s^{-1} from Han & Mould (1992). At small redshifts, the H_0 is related to the distance modulus by $(m-M) = 25 + 5\log(cz/H_0) + 1.086(1-q_0)z$. The last term accounts for cosmological curvature, and its effect on H_0 is negligible: $\leq 2\%$ at the redshift of Coma for q_0 ranging from –1 to +1. Our resulting Hubble constant is 71 ± 8 km s^{-1} Mpc^{-1}.

Keck Observatory was made possible by the generous support of the W. M. Keck Foundation. We thank the staffs of Lick and Keck Observatories for their help, especially Chuck Sorenson, Wendy Harrison, and Wayne Earthman. We also thank Bill Harris and J.J. Kavelaars for making their NGC 4874 results available. This research was supported by NSF grant no. AST-9617173 and *HST* NASA grant no. GO-07458.01-96A to the authors. M. Liu is also grateful for support from the Beatrice Watson Parrent Fellowship at the University of Hawai'i.

REFERENCES

Abell, G. O. 1958, ApJS, 3, 211
Baier, F. W., Fritze, K., & Tiersch, H. 1990, Astronomische Nachrichten, 311, 89
Barmby, P., Huchra, J. P., Brodie, J. P., Forbes, D. A., Schroder, L. L., & Grillmair, C. J. 2000, AJ, 119, 727
Bershady, M. A., Lowenthal, J. D., & Koo, D. C. 1998, ApJ, 505, 50
Blakeslee, J. P., Ajhar, E. A., & Tonry, J. L. 1999, in Post-Hipparcos Cosmic Candles, ed. A. Heck & F. Caputo (Dordrecht: Kluwer), 181
Blakeslee, J. P. & Tonry, J. L. 1995, ApJ, 442, 579
Capaccioli, M., Cappellaro, E., della Valle, M., D'Onofrio, M., Rosino, L., & Turatto, M. 1990, ApJ, 350, 110
Casali, M. M. & Hawarden, T. G. 1992, JCMT-UKIRT Newsletter, 4, 33
Colless, M. & Dunn, A. M. 1996, ApJ, 458, 435
Davis, D. S. & Mushotzky, R. F. 1993, AJ, 105, 409
de Vaucouleurs, G., de Vaucouleurs, A., Corwin, H. G., Buta, R. J., Paturel, G., & Fouque, P. 1991, Third Reference Catalogue of Bright Galaxies (Springer-Verlag)
D'Onofrio, M., Capaccioli, M., Zaggia, S. R., & Caon, N. 1997, MNRAS, 289, 847
Ferrarese, L., Ford, H. C., Huchra, J., Kennicutt, R. C., Mould, J. R., Sakai, S., Freedman, W. L., Stetson, P. B., Madore, B. F., Gibson, B. K., Graham, J. A., Hughes, S. M., Illingworth, G. D., Kelson, D. D., Macri, L., Sebo, K., & Silbermann, N. A. 2000, ApJS, 128, 431
Freedman, W. et al. 2001, ApJ, in press (astro-ph/0012376)
Frogel, J. A., Persson, S. E., Matthews, K., & Aaronson, M. 1978, ApJ, 220, 75
Gilmore, K., Rank, D., & Temi, P. 1995, in IAU Symp. 167: New Developments in Array Technology and Applications, Vol. 167, 79
Giovanelli, R., Haynes, M. P., Salzer, J. J., Wegner, G., da Costa, L. N., & Freudling, W. 1998, AJ, 116, 2632
Han, M. & Mould, J. R. 1992, ApJ, 396, 453
Harris, W. E. 1987, ApJ, 315, L29
Harris, W. E., Kavelaars, J. J., Hanes, D. A., Hesser, J. E., & Pritchet, C. J. 2000, ApJ, 533, 137
Jacoby, G. H., Branch, D., Clardullo, R., Davies, R. L., Harris, W. E., Pierce, M. J., Pritchet, C. J., Tonry, J. L., & Welch, D. L. 1992, PASP, 104, 599
Jensen, J. B., Tonry, J. L., & Luppino, G. A. 1998, ApJ, 505, 111
—. 1999, ApJ, 510, 71
Jensen, J. B., Tonry, J. L., Thompson, R. I., Ajhar, E. A., Lauer, T. R., Rieke, M. J., Postman, M., & Liu, M. C. 2001, ApJ, 550, 503
Jorgensen, I., Franx, M., & Kjaergaard, P. 1995, MNRAS, 276, 1341
Kavelaars, J. J., Harris, W. E., Hanes, D. A., Hesser, J. E., & Pritchet, C. J. 2000, ApJ, 533, 125
Liu, M. C. 2000, PhD thesis, University of California, Berkeley
Liu, M. C., Charlot, S. ., & Graham, J. R. 2000, ApJ, 543, 644
Liu, M. C., Graham, J. R., & Charlot, S. 2001, ApJ, in press (astro-ph/0107357)
Luppino, G. A. & Tonry, J. L. 1993, ApJ, 410, 81
Matthews, K. & Soifer, B. 1994, in Infrared Astronomy with Arrays: The Next Generation, ed. I. McLean (Dordrecht: Kluwer), 239
McLeod, B. A., Bernstein, G. M., Rieke, M. J., Tollestrup, E. V., & Fazio, G. G. 1995, ApJS, 96, 117
Mei, S., Silva, D. R., & Quinn, P. J. 2001, A&A, 366, 54
Mohr, J. J., Fabricant, D. G., & Geller, M. J. 1993, ApJ, 413, 492
Pahre, M. A. & Mould, J. R. 1994, ApJ, 433, 567
Persson, S. E., Frogel, J. A., & Aaronson, M. 1979, ApJS, 39, 61
Pickles, A. J. 1998, PASP, 110, 863
Schlegel, D. J., Finkbeiner, D. P., & Davis, M. 1998, ApJ, 500, 525
Strauss, M. A. & Willick, J. A. 1995, Phys. Rep., 261, 271
Thomsen, B., Baum, W. A., Hammergren, M., & Worthey, G. 1997, ApJ, 483, L37
Tonry, J. L., Ajhar, E. A., & Luppino, G. A. 1990, AJ, 100, 1416 (erratum AJ, 101, 1942)
Tonry, J. L. et al. 2000, ApJ, in press
Wainscoat, R. J. & Cowie, L. L. 1992, AJ, 103, 332
White, S. D. M., Briel, U. G., & Henry, J. P. 1993, MNRAS, 261, L8

TABLE 1

NGC 4874 K-BAND SBF MEASUREMENTS

Date	t_{int} (s)	Radius ($''$)	$\langle\mu_K\rangle$[a] (mag/$\Box''$)	$V-I_c$[a] (mag)	P_{GC}/P_0[b]	P_{sky}/P_0[b]	$(P_0-P_r)/P_1$[c]	$\overline{m}_K$[d] (mag)
18 Mar 1995	1920	3–9	16.68	1.219 ± 0.015	0.00 ± 0.13	0.69 ± 0.17	6.7 ± 1.4	29.52 ± 0.32
19 Mar 1998	3600	3–9	16.68	1.219 ± 0.015	0.00 ± 0.14	0.48 ± 0.20	9.3 ± 2.2	29.47 ± 0.22
19 Mar 1998	3600	9–12	17.49	1.198 ± 0.015	0.00 ± 0.10	0.58 ± 0.16	7.2 ± 1.3	29.18 ± 0.24

[a]Mean K-band surface brightness and $V-I_c$ color of the region used for SBF measurement. The $V-I_c$ data are from Harris et al. (2000) and have had k-corrections applied.

[b]The fractional contamination to the total SBF signal P_0. P_{GC} is the variance from globular clusters which are undetected in the *HST* optical imaging. P_{sky} is the variance measured from images of blank sky, which arises from instrumental noise and unresolved background galaxies. Both P_{GC} and P_{sky} are normalized to the mean surface brightness in the measurement region. The quoted errors include the error in P_0, which dominates the error in P_{GC}/P_0.

[c]The signal-to-noise of the stellar SBF signal. P_r is the total residual variance and is the sum of P_{GC} and P_{sky}. The difference (P_0-P_r) is the stellar SBF variance. P_1 measures photon shot noise, the flat component of the power spectra plots.

[d]The final SBF apparent magnitudes. The values have been corrected for extinction and have had k-corrections applied.